

An active temperature compensated fiber Bragg grating vibration sensor for high-temperature application

CHEN Bao-jie^{1,2}, JIA Ping-gang^{1,2}, QIAN Jiang^{1,2}, FENG Fei^{1,2},
HONG Ying-ping^{1,2}, LIU Wen-yi^{1,2}, XIONG Ji-jun^{1,2}

(1. Key Laboratory of Instrumentation Science and Dynamic Measurement (North University of China),
Ministry of Education, Taiyuan 030051, China;

2. Science and Technology on Electronic Test & Measurement Laboratory, North University of China, Taiyuan 030051, China)

Abstract: An active temperature compensated fiber Bragg grating (FBG) vibration sensor with a constant section cantilever beam is proposed for the simultaneous measurement of temperature and vibration, and the sensor is verified by a temperature compensation feedback system. The high-temperature vibration sensor is composed of a quartz cantilever beam and a femtosecond Bragg grating. The feedback control demodulation system of active temperature compensation can adjust the laser wavelength to stabilize the grating offset point and realize simultaneous measurement of temperature and vibration. On this basis, the performance of the sensor is tested and analyzed within the range of 20–400 °C by setting up a high-temperature vibration test system. The experimental results show that the sensitivity of the sensor is about 132.33 mV/g, and the nonlinearity is about 3.33%. The sensitivity between the laser wavelength and temperature is about 0.013 07 nm/°C. In addition, the active temperature compensated fiber Bragg grating vibration sensor has the advantages of a simple structure, stable performance, easy demodulation and high sensitivity. Moreover, the sensor can achieve high temperature vibration signal monitoring and has good practical application value.

Key words: fiber Bragg grating (FBG); vibration sensor; active temperature compensation; cantilever beam; feedback control

CLD number: TP273

doi: 10.3969/j.issn.1674-8042.2020.04.012

0 Introduction

Measurement of vibrations in harsh environments is of great significance for the monitoring of parameters such as bridge construction, oil well extraction, biomedicine, power industry, aircraft engines and so on^[1-4]. At present, high-temperature vibration sensors commonly used in engineering applications mainly include magnetoelectric vibration sensors, piezoresistive vibration sensors, capacitive vibration sensors, piezoelectric vibration sensors and optical vibration sensors^[5-9]. Compared with the traditional electrical vibration sensor, the optical sensors have the characteristics of small volume, light weight and good anti electromagnetic interference ability, which is especially suitable for the measurement of physical quantities in a strong magnetic field or during exposure to radiation, corrosion, high temperatures and other environments^[10-12]. Because fiber has many

advantages in sensing, the sensing technology of the fiber Bragg grating (FBG) has also been researched and developed.

FBG vibration sensors mainly include the simple beam FBG vibration sensor, the non-contact FBG vibration sensor and the equal strength beam FBG high/low frequency vibration sensor^[13-15]. Because it has advantages of small size, embeddability, multi-point distributed measurement, reusability and so on, it has attracted significant attention in many industries.

In recent years, there has been some research and exploration on fiber grating vibration sensors. Casas-Ramos et al developed a cantilever beam FBG vibration sensor based on the axial property of the FBG with a sensitivity of 339 pm/g^[16]. Satoshi et al designed a fiber-optic mechanical vibration sensor that uses a lead piezoelectric geophone (LPG) as a sensing element, which has a dynamic response range

Received date: 2020-05-19

Foundation items: National Natural Science Foundation of China (No. 51935011); Natural Science Foundation of Shanxi Province of China (No. 201901D111160); Innovative Research Group Project of National Science Foundation of China (No. 51821003)

Corresponding author: XIONG Ji-jun (xiongjijun@nuc.edu.cn)

of 90 dB^[17]. Zhang et al designed a new type of special structure vibration sensor based on the FBG with a measurement range of 0 Hz – 100 Hz^[18]. Khan et al studied a FBG accelerometer based on L-shaped cantilever, with a sensitivity of 306 pm/g under 150 Hz frequency^[19]. However, the FBG vibration sensors studied currently cannot meet the test requirements in a high-temperature environment, and FBG sensors will have a temperature coupling phenomenon in high-temperature environments, which reduces their measurement accuracy^[20-21].

Based on these factors, a high-temperature resistant vibration sensor which uses quartz as a cantilever beam and the femtosecond Bragg grating as a sensing element is proposed in this paper. We adopt a demodulation method for the active feedback control system which can adjust the laser wavelength to stabilize the grating offset point to test the performance of the high-temperature fiber grating vibration sensor. Moreover, a proportional-integral-derivative (PID) feedback control system is used to control the laser wavelength in real time, which can not only demodulate the vibration signal, but also eliminate the influence of temperature on the grating drift^[22-23]. The performance of the sensor is tested and analyzed within the range of 20 °C – 400 °C by setting up a high-temperature vibration test system.

1 Sensing principle

The structure of the active temperature compensated FBG vibration sensor is shown in Fig. 1.

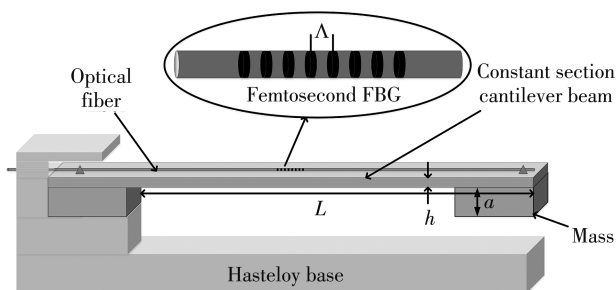


Fig. 1 Schematic diagram of vibration sensor

The femtosecond FBG is bonded to a full quartz constant section cantilever beam (length: 20 mm, width: 5 mm, thickness: 0.2 mm) with a quartz mass (length: 5 mm, width: 5 mm, thickness: 1 mm) on the surface of the free end. At the other end of the constant section, the quartz cantilever beam integrated with the mass at the free end is fixed to the Hastelloy base to form a mass-spring-damper

system. The length of the femtosecond FBG is 3 mm. When the FBG is excited by the acceleration in the vertical direction of the cantilever beam, the mass generates relative movement under the action of the inertial force, so that the reflection spectrum signal of the femtosecond FBG changes accordingly. The constant section cantilever beam structure is analyzed and the periodic variation in the intensity of the grating's spectral signal is obtained, allowing the measurement of the vibration signal.

In a constant section cantilever structure, when the cantilever with fiber grating is excited by the acceleration along the vertical direction of the cantilever, the structure of the sensor can be simplified as a single degree of freedom forced vibration system. If the influence of the volume of the mass on the deflection of the cantilever beam is ignored, the strain on the surface of the constant section cantilever beam with mass at the free end can be expressed as

$$\epsilon_x = \frac{6F(L-x)}{Ebh^2}, \quad (1)$$

where E is the elastic modulus; F is the force on the inertial mass; x is the distance from any point on the cantilever to the fixed end; L , b and h are the length, width, and thickness of the constant section cantilever beam, respectively.

When the external physical quantity acts on the fiber grating, the center wavelength of the grating drifts, which can be expressed as

$$\frac{\Delta\lambda_B}{\lambda_B} = \frac{\Delta n_{\text{eff}}}{n_{\text{eff}}} + \frac{\Delta\Lambda}{\Lambda} = (1 - P_e)\epsilon_x, \quad (2)$$

where n_{eff} is the effective refractive index of the fiber core, Λ is the period of the fiber grating, P_e is the effective elastic coefficient of the fiber grating, ϵ_x is the strain at any point on the cantilever, and λ_B is the center wavelength of the fiber grating.

Therefore, the change in the center wavelength of the Bragg grating at any point on the cantilever can be expressed as

$$\Delta\lambda = (1 - P_e) \frac{6F(L-x)}{Ebh^2}. \quad (3)$$

According to Newton's second law, Eq. (3) can be expressed as

$$\Delta\lambda = (1 - P_e) \frac{6m(L-x)}{Ebh^2}, \quad (4)$$

where m is the equivalent mass of the mass-spring-damper system. From Eq. (4), it can be seen that

acceleration is linear related to the wavelength change of the fiber grating.

When the fiber grating is subjected to temperature change, the drift of the central wavelength of the FBG can be expressed as^[24]

$$\frac{\Delta\lambda_B}{\lambda_B} = \left(\frac{1}{n_{\text{eff}}} \times \frac{\partial n_{\text{eff}}}{\partial T} + \frac{1}{\Lambda} \times \frac{\partial \Lambda}{\partial T} \right) \Delta T, \quad (5)$$

where $\Delta\lambda_B$ is the change in the center wavelength of the fiber grating, Δn_{eff} is the change in the refractive index of the core, $\Delta\Lambda$ is the change in the period of the fiber grating grid, and ΔT is the change in temperature. Therefore, the fiber grating can be calibrated before the experimental test, and then the sensitivity of the central wavelength with temperature can be obtained based on Eq. (4), so that the influence of temperature on the fiber grating can be detected. The active feedback system and PID control can be used to stabilize the offset point of the FBG to compensate for the temperature.

The principle diagram of grating intensity demodulation is shown in Fig. 2.

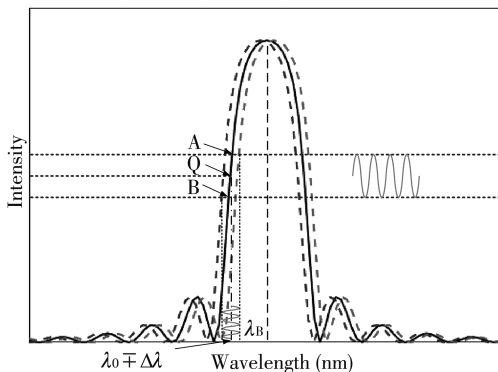


Fig. 2 Demodulation schematic

Due to the small change in the grating caused by acceleration, it can be regarded as a linear change of light intensity in a small wavelength range; that is, FBG is subject to uniform strain. Then, the wavelength bar of the tunable laser is adjusted to the offset point of the FBG, that is, the position of the wavelength (λ_0) corresponding to point Q in the linear part of the reflection spectrum. When the vibration signal causes the reflection spectrum to shift, the reflected light intensity changes accordingly, and vibration information is obtained by detecting the change in light intensity. Considering that the intensity between the reflection spectra A and B is linear, and the slope at the wavelength (λ_0) position at point Q is k , then the spectral shift is $\Delta\lambda$ under the acceleration. At the same time, the change in reflected light intensity is

$$\Delta I = k\Delta\lambda. \quad (6)$$

The corresponding light intensity signal is converted into a voltage output signal through a photodetector (Model 2053, New Focus, San Jose, CA, America), that is, the output voltage change is

$$\Delta V = D\eta\Delta I, \quad (7)$$

where D is the product of the photodetector wavelength influence factor and the magnification factor η is the attenuation coefficient of light in the system.

From Eqs. (3), (6), (7) and Newton's second law, the output voltage change is given as

$$\Delta V = kD\eta(1 - P_c) \frac{6F(L - x)}{Ebh^2}. \quad (8)$$

2 System construction and experimental test

A schematic diagram of the active temperature compensated FBG vibration sensor test system based on the constant section cantilever beam is shown in Fig. 3. A high-temperature experimental device was set up to calibrate and test the FBG vibration sensor in real time. This experimental setup consisted of a ThermConcept (GSL-1100X-S, HF kejing, Hefei, China), a sensing and demodulation system, and a vibration calibration system. In the vibration calibration system, the signal generator and power amplifier controlled the vibration exciter (TV 50101, Tira, Thuringen, Germany) to apply the required vibration signal to the sensor. The high-temperature ThermConcept was fixed vertically above the vibration exciter, providing a high-temperature working environment for the sensor. In the sensing and demodulation system, when the tunable laser (GM82009, Guilin GM Technology Industry Ltd, Guilin, China) light source emitted a beam, it passed through the coupler (1310/1550-SSC) to the sensor and demodulation system. The FBG vibration sensor with Hastelloy base was fixed to the top of the quartz rod, and together put into the ThermConcept. The quartz rod was connected to the vibration exciter. Another path of light was reflected back through the photodetector and the feedback system to demodulate the vibration signal. Afterwards, the data passed through the data acquisition technology (USB2833, Beijing ART Technology, Beijing, China) and the PID feedback control module was established based on Labview software on the host computer to control

the laser wavelength automatically. Continuous tracking deviation of the center wavelength stabilized the grating offset point and the use of a photodetector

obtained the change in light intensity in the liner region. Thus real-time monitoring of temperature and vibration signals was finally achieved.

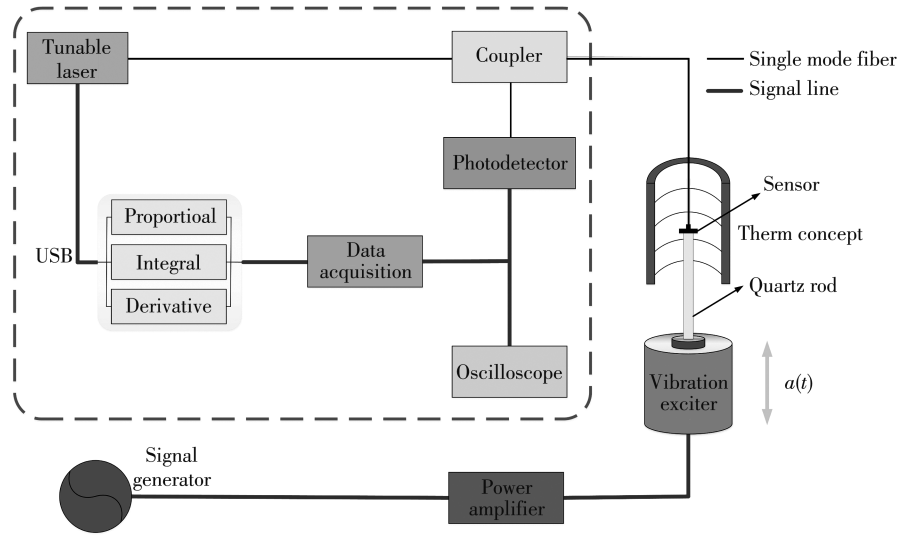
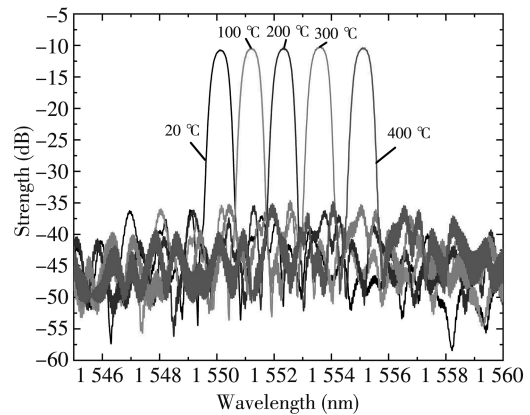


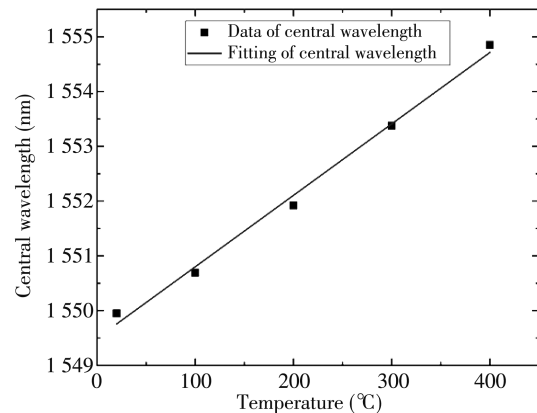
Fig. 3 High-temperature FBG vibration sensor test system

2.1 Temperature experiment and test results

In order to analyze the influence of temperature on the FBG, the temperature drift of the FBG was tested under static conditions. At the beginning of the experiment, the obtained initial central wavelength of the FBG sensor was 1 549. 905 nm by an optical analyzer (Micron Optics Inc., SM125, America) at 20 °C, and then the temperature was increased from 20 °C to 400 °C with an increment of 100 °C by using a ThermConcept. Each temperature was maintained for 10 min, and we tested the corresponding spectrum signals after the temperature stabilized. Then, the central wavelength of the fiber grating was analyzed and demodulated by Micron Optics Inc. (MOI) under static conditions, and the change value of the central wavelength was recorded at 20 °C, 100 °C, 200 °C, 300 °C and 400 °C, respectively. Fig. 4(a) shows the optical spectrogram of the sensing fiber grating at different temperatures measured by the optical analyzer. It can be seen that the spectral signal of FBG demonstrates a shift phenomenon with a rise in temperature, that is, it moves in the long wavelength direction. Fig. 4(b) shows the change in the central wavelength of the fiber grating with temperature. Through fitting, we found that the temperature drift coefficient is 0. 013 05 nm/°C, and the correlation coefficient R^2 is 0. 993 46.



(a) Spectral diagram of FBG changes with temperature



(b) Relationship of FBG central wavelength changes with temperature

Fig. 4 Temperature drift diagram of femtosecond FBG

In order to eliminate the influence of temperature drift, as the temperature of the sensor increased in

the high-temperature vibration experiment, the laser wavelength was controlled by PID feedback to stabilize the offset point of the grating, thereby achieving the effect of temperature compensation for the sensor. When the laser was working normally, we obtained the relationship between the working wavelength of the laser and the temperature at 20 °C, 100 °C, 200 °C, 300 °C and 400 °C, respectively. As shown in Fig. 5, after feedback control, the laser wavelength and temperature demonstrate a linear relationship. The linear relationship has an R^2 value of 0.999 14, and the temperature sensitivity of the sensor is 0.013 07 nm/°C.

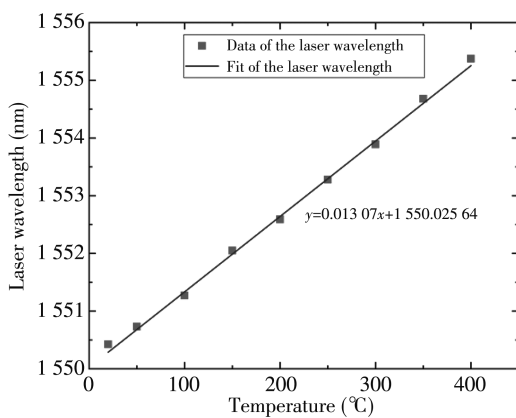
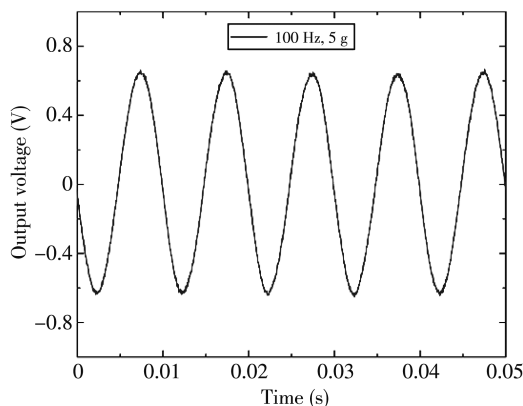


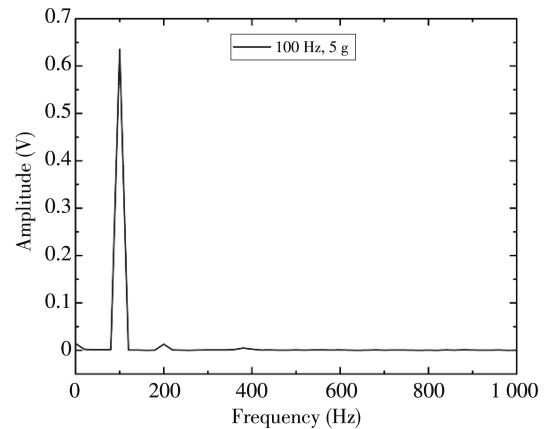
Fig. 5 Relationship between sensor temperature and laser wavelength controlled by PID feedback

2.2 Vibration experiment and results

In the vibration experiment test, the sensor was heated from 20 °C to 400 °C with an increment of 100 °C by a high-temperature ThermConcept, and the vibration signals were tested at different vibration accelerations from 0 g to 8 g. We tested vibration signal of the sensor at a frequency of 100 Hz and an acceleration of 5 g. The output signal and frequency response of the sensor are shown in Fig. 6.



(a) Waveform graph of output voltage over time



(b) Fast Fourier transform spectrum of waveform

Fig. 6 Vibration signals and frequency responses at 100 Hz and 5 g

It can be seen from Fig. 6(a) that the sensor can output a stable sinusoidal vibration signal at 100 Hz. According to the peak-peak voltage value of the waveform, the voltage sensitivity of the system is about 132.33 mV/g. It can be seen from Fig. 6(b) that the sensor has a good frequency response under 100 Hz frequency, which is in good agreement with the frequency of the vibration exciter.

At a room temperature of 20 °C, we performed three repeatability tests to verify the stability of the sensor. The test results are shown in Fig. 7. It can be seen that the amplitude voltage of the sensor output gradually increases with the acceleration value. After calculation and fitting, the three curves basically coincide, and the repeatability error and nonlinear error of the vibration sensitivity of the sensor are about 2.8% and less than 1.55%, respectively.

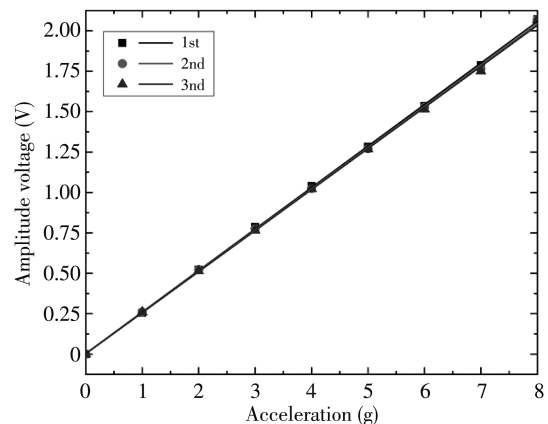


Fig. 7 Vibration repeatability diagram at room temperature

In the high-temperature vibration experiment, the temperature of ThermConcept was increased from 20 °C to 400 °C with an increment of 100 °C. When the temperature is stable for a period of time, the vibration signal was measured at a frequency of

100 Hz, and the acceleration value was from 0 g to 8 g. The output signal of the vibration sensor changed during the with acceleration. The linearity curve of the amplitude voltage and acceleration is shown in Fig. 8 where the center wavelength of FBG drifted with the change in temperature. The central wavelength was measured after red shift as the new central wavelength, and the offset point of FBG was searched again by the automatic feedback control system to demodulate the vibration signal, so as to reduce the influence of temperature on the central wavelength of the fiber grating. From Fig. 8, we can see that the minimum nonlinearity of the vibration signal is 3.33% under high-temperatures.

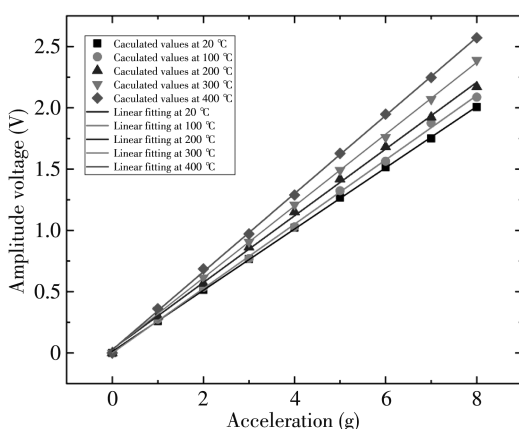


Fig. 8 Relationship between acceleration and amplitude voltage at different temperatures

In the high-temperature vibration sensing test, the vibration signal and temperature were measured by the change in the bias point of the grating at the same time. However, the offset point can be affected by the temperature, therefore the temperature feedback control system was used to correct the offset point. For FBG, the increase in temperature will change the period of the grating, so that the spectrum of the fiber grating appears to have a red shift with the change of temperature; that is to say, it moves in the long wavelength direction. When testing vibration signals at high-temperatures, the temperature will affect the sensitivity of the sensor. The sensitivity versus temperature curve of the vibration signals measured at different temperatures is shown in Fig. 9. It can be seen that the sensitivity of the sensor decreases as the temperature increases, and the linear relationship has an R^2 value of 0.989 83.

It can be seen from Fig. 4(b) that the central wavelength of the fiber grating increases as the temperature increases, and its correlation coefficient (R^2) is 0.993 46. According to the measured

temperature and the relationship with sensitivity shown in Fig. 9, the offset point and sensitivity of the sensor were corrected to achieve temperature decoupling. The measured acceleration value and standard acceleration value at 20 °C, 100 °C, 200 °C, 300 °C and 400 °C with decoupling are shown in Fig. 10. The maximal error of the acceleration after temperature decoupling is less than 3.33% within the acceleration range of 0 g – 8 g. After temperature decoupling of the sensor, the measured acceleration of the sensor is basically the same as the standard acceleration, and the experiment proves that the sensor is practical and reliable.

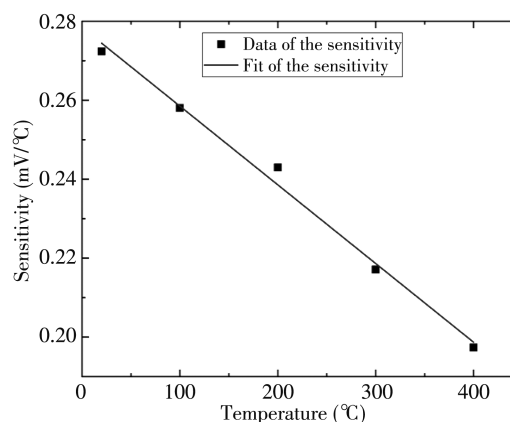


Fig. 9 Sensitivity drift diagram with temperature

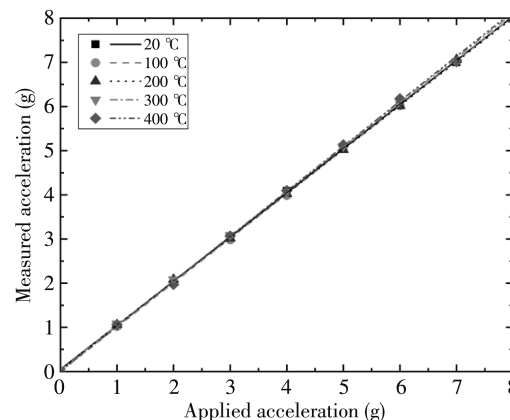


Fig. 10 Acceleration measurement results after temperature decoupling

3 Conclusion

In this paper, an active temperature compensated FBG vibration sensor with a quartz constant section cantilever beam was introduced, and the temperature and vibration signals were studied experimentally by the active temperature compensation method using the PID automatic control laser wavelength. The performance of the sensor was tested and analyzed within the temperature range of 20 °C – 400 °C by setting up a high-temperature vibration test system.

The experimental results show that the acceleration sensitivity of the vibration sensor is about 132.33 mV/g, and the nonlinearity is about 3.33%. The laser wavelength was controlled by PID feedback to stabilize the offset point of the grating for temperature compensation. The sensitivity of the laser wavelength and temperature is about 0.01307 nm/°C, and the correlation coefficient (R^2) is about 0.99914. In conclusion, the active temperature compensated FBG vibration sensor has a stable sensing performance, easy demodulation, simple structure and a higher sensitivity. Moreover, the sensor is suitable for online monitoring of vibration signals at high-temperatures and has good practical application value.

References

- [1] Vohra S, Johnson G, Todd M, et al. Distributed strain monitoring with arrays of fiber Bragg grating sensors on an in-construction steel box-girder bridge. *IEICE transactions on Electronics*, 2000, 83(3): 454-461.
- [2] Sohn K R, Shim J H. Liquid-level monitoring sensor systems using fiber Bragg grating embedded in cantilever. *Sensors and Actuators A: Physical*, 2009, 152(2): 248-251.
- [3] Rao Y J. Recent progress in applications of in-fibre Bragg grating sensors. *Optics and Lasers in Engineering*, 1999, 31(4): 297-324.
- [4] Neumann M, Dreier F, Günther P, et al. A laser-optical sensor system for blade vibration detection of high-speed compressors. *Mechanical Systems and Signal Processing*, 2015, 64: 337-346.
- [5] Salzer S, Jahns R, Piorra A, et al. Tuning fork for noise suppression in magnetoelectric sensors. *Sensors and Actuators A: Physical*, 2016, 237: 91-95.
- [6] Kon S, Oldham K, Horowitz R. Piezoresistive and piezoelectric MEMS strain sensors for vibration detection. In: *Proceedings of Sensors and Smart Structures Technologies for Civil, Mechanical, and Aerospace Systems 2007*, International Society for Optics and Photonics, 2007: 6529.
- [7] Kim K, Zhang S, Salazar G, et al. Design, fabrication and characterization of high temperature piezoelectric vibration sensor using YCOB crystals. *Sensors and Actuators A: Physical*, 2012, 178: 40-48.
- [8] Abarca-Jiménez G S, Reyes-Barranca M A, Mendoza-Acevedo S, et al. Modal analysis of a structure used as a capacitive MEMS accelerometer sensor. In: *Proceedings of 2014 11th International Conference on Electrical Engineering, Computing Science and Automatic Control (CCE)*, IEEE, 2014: 1-4.
- [9] Zhang Z, Bao X. Distributed optical fiber vibration sensor based on spectrum analysis of polarization-OTDR system. *Optics Express*, 2008, 16(14): 10240-10247.
- [10] James S W, Tatam R P. Optical fibre long-period grating sensors: characteristics and application. *Measurement Science and Technology*, 2003, 14(5): R49.
- [11] Wada A, Tanaka S, Takahashi N. Optical fiber vibration sensor using FBG Fabry-Perot interferometer with wavelength scanning and Fourier analysis. *IEEE Sensors Journal*, 2011, 12(1): 225-229.
- [12] He T, Ran Y, Liu T, et al. Distributed temperature/vibration fiber optic sensor with high precision and wide bandwidth. *IEEE Photonics Journal*, 2019, 11(6): 1-11.
- [13] Lan L, Dong X Y, Zhao C L, et al. Simply-supported beam-based fiber Bragg grating vibration sensor. *Infrared and Laser Engineering*, 2011, 40(12): 2497-2500.
- [14] Li T, Tan Y, Zhou Z, et al. Study on the non-contact FBG vibration sensor and its application. *Photonic Sensors*, 2015, 5(2): 128-136.
- [15] Chah K, Caucheteur C, Mégret P, et al. Reflective polarimetric vibration sensor based on temperature-independent FBG in HiBi microstructured optical fiber. In: *proceedings of Optical Sensing and Detection III*, International Society for Optics and Photonics, 2014: 9141.
- [16] Casas-Ramos M A, Sandoval-Romero G E. Cantilever beam vibration sensor based on the axial property of fiber Bragg grating. *Smart Structures and Systems*, 2017, 19(6): 625-631.
- [17] Tanaka S, Somatomo H, Wada A, et al. Fiber-optic mechanical vibration sensor using long-period fiber grating. *Japanese Journal of Applied Physics*, 2009, 48(7S): 07GE05.
- [18] Zhang Z Z, Liu C T. Design of vibration sensor based on fiber bragg grating. *Photonic Sensors*, 2017, 7(4): 345-349.
- [19] Khan M M, Panwar N, Dhawan R. Modified cantilever beam shaped FBG based accelerometer with self temperature compensation. *Sensors and Actuators A: Physical*, 2014, 205: 79-85.
- [20] Zhang L C, Jiang Y, Jia J S. Fiber-optic micro vibration sensors fabricated by a femtosecond laser. *Optics and Lasers in Engineering*, 2018, 110: 207-210.
- [21] Wang X F, Guo Y X, Xiong L. Hybrid fiber Bragg grating sensor for vibration and temperature monitoring of a train bearing. *Chinese Optics Letters*, 2018, 16(7): 27-32.
- [22] Hamid N H A, Kamal M M, Yahaya F H. Application of PID controller in controlling refrigerator temperature. In: *proceedings of 5th International Colloquium on Signal Processing & its Applications*, IEEE, 2009: 378-384.
- [23] Ren F F, Zhang W F, Li Y W. The Temperature Compensation of FBG Sensor for Monitoring the Stress on Hole-Edge. *IEEE Photonics Journal*. 2018, 10(4): 1-9.
- [24] Rao Y J. *Fiber Bragg grating sensors: principles and applications*. Optical Fiber Sensor Technology, Springer, Boston, MA, 1998: 355-379.

基于主动温度补偿的高温光纤布拉格光栅振动传感器

陈宝杰^{1,2}, 贾平岗^{1,2}, 钱江^{1,2}, 冯飞^{1,2}, 洪应平^{1,2}, 刘文怡^{1,2}, 熊继军^{1,2}

(1. 中北大学 仪器科学与动态测试教育部重点实验室, 山西 太原 030051;

2. 中北大学 电子测试技术重点实验室, 山西 太原 030051)

摘要: 提出了一种基于主动温度补偿的等截面悬臂梁式光纤布拉格光栅(FBG)振动传感器, 可用于同时测量温度和振动, 并通过温度补偿反馈解调系统对该传感器进行了实验验证。该高温振动传感器由石英悬臂梁和飞秒布拉格光栅组成。采用了主动温度补偿的反馈控制解调系统, 可以不断地调节激光波长来稳定光栅偏置点, 并实现温度和振动的同时测量。在此基础上, 通过搭建高温振动测试系统, 在 20—400 °C 的温度范围内对传感器的性能进行测试和分析。实验结果表明传感器的灵敏度约为 132.33 mV/g, 线性度约为 3.33%, 激光波长与温度之间的灵敏度约为 0.013 07 nm/°C。另外, 该主动温度补偿光纤布拉格光栅振动传感系统具有结构简单, 性能稳定, 易于解调, 灵敏度高的优点。该传感器可以实现高温振动信号的监测, 具有良好的实际应用价值。

关键词: 布拉格光栅; 振动传感器; 主动温度补偿; 悬臂梁; 反馈控制

引用格式: CHEN Bao-jie, JIA Ping-gang, QIAN Jiang, et al. An active temperature compensated fiber Bragg grating vibration sensor for high-temperature application. *Journal of Measurement Science and Instrumentation*, 2020, 11(4): 397-404. [doi: 10.3969/j.issn.1674-8042.2020.04.012]